ORNL/TM-2015/627

Synthesis and Luminescence Characteristics of Cr^{3+} doped $Y_3Al_5O_{12}$ Phosphors

Case Collins
Reza T. Dabestani
Tolga Aytug
Cyril V. Thompson
Linda A. Lewis
Brenda A. Smith

October 2015

OAK RIDGE NATIONAL LABORATORY
MANAGED BY UT-BATTELLE FOR THE US DEPARTMENT OF ENERGY

ORNL/TM-2015/627

Chemical Sciences Division

SYNTHESIS AND LUMINESCENCE CHARACTERISTICS OF CR^{3+} DOPED $Y_3AL_5O_{12}$ PHOSPHORS

Case Collins
Reza T. Dabestani
Tolga Aytug
Cyril V. Thompson
Linda A. Lewis
Brenda A. Smith

Date Published: October 2015

Prepared by
OAK RIDGE NATIONAL LABORATORY
Oak Ridge, Tennessee 37831-6283
managed by
UT-BATTELLE, LLC
for the
US DEPARTMENT OF ENERGY
under contract DE-AC05-00OR22725

CONTENTS

Page

LIST OF FIGURES

Figure **Page**

ACRONYMS

CL	Cathodoluminescence
DP	Direct-Precipitation
DTRA	Defense Threat Reduction Agency
HP	Hydrothermal-Precipitation
ICDD	International Center for Diffraction Data
LED	Light-Emitting Diode
ORNL	Oak Ridge National Laboratory
PDF	Portable Document Format
PL	Photoluminescence
RHEED	Reflected High Energy Electron Diffraction
XRD	X-Ray Diffraction
YAG	Yttrium Aluminum Garnet ($Y_3Al_5O_{12}$)
YAM	Yttrium Aluminum Monoclinic ($Y_4Al_2O_9$)
YAP	Yttrium Aluminum Perovskite ($YAlO_3$)
WDTS	Workforce Development for Teachers and Scientists

ACKNOWLEDGMENTS

This work was supported by the Defense Threat Reduction Agency (DTRA) / J9 Basic Research. The internship (C. Collins) was supported by the U.S. Department of Energy, Office of Science, Office of Workforce Development for Teachers and Scientists (WDTS) under the Science Undergraduate Laboratory Internship program.

ABSTRACT

Luminescence performance of yttrium aluminum garnet ($Y_3Al_5O_{12}$) phosphors as a function of Cr^{3+} concentration has been investigated via two different wet-chemical synthesis techniques, direct- (DP) and hydrothermal-precipitation (HP). Using either of these methods, the red-emitting phosphor [$Y_3Al_{5-x}Cr_xO_{12}$ (YAG: Cr^{3+})] showed similar photoluminescence (PL) intensities once the dopant concentration was optimized. Specifically, the YAG: Cr^{3+} PL emission intensity reached a maximum at Cr^{3+} concentrations of x = 0.02 (0.4 at.%) and x = 0.13 (2.6 at.%) for DP and HP processed samples, respectively. The results indicated the strong influence of the processing method on the optimized YAG: Cr^{3+} performance, where a more effective energy transfer rate between a pair of Cr^{3+} activators at low concentration levels was observed by using the DP synthesis technique. Development of a highly efficient phosphor, using a facile synthesis approach, could significantly benefit consumer and industrial applications by improving the operational efficiency of a wide range of practical devices.

1.0 INTRODUCTION

A phosphor-based white light emitting diode (LED) consists of a LED coated with a phosphor, where the light emitted from the LED and phosphor produces a broad emission spectrum that is observed as white light. To improve the phosphor-based white light emitting diode's luminous efficiency, an LED can be coated with multi-layers/blends of phosphors exhibiting distinct colors (e.g. blue, green, yellow, and red). For instance by combining different monochromatic light sources (e.g. red, green, and blue) on an LED, the emitted white light spectrum can be broadened even further.[1] By enhancing the luminous efficiency, these light emitting phosphors can become more energy efficient and one day replace current conventional lighting sources, such as incandescent, linear fluorescent, and metal halide bulbs.[2] Such phosphors are not only applicable to LEDs but also have great potential in applications where solid-state lasers and cathode ray tubes (CRTs) are utilized.[3] The strong broad red luminescence of the $Y_3Al_{5-x}Cr_xO_{12}$ is appealing for such applications.

The luminescent efficiency of the $Y_3Al_5O_{12}$ (YAG – yttrium aluminum garnet) phosphor is dependent upon the purity of the YAG composition. Before obtaining the optimum highly luminescent garnet phase, two intermediate phases of $Y_4Al_2O_9$ (YAM – yttrium aluminum monoclinic) and $YAlO_3$ (YAP – yttrium aluminum perovskite) can form within the material system. If any of the YAM and YAP phases coexist with the final product, the luminescent emission is substantially diminished.

There are many well-known synthetic methods in preparing YAG phosphors.[4] The solid-state reaction method is a common approach for synthesizing a YAG phosphor.[5] The major disadvantage of using this method is that it often requires extensive precursor milling and high sintering temperatures (≥1600 °C). While an increased homogeneity of starting materials can be obtained by extensive milling, reproducibility of the desired stoichiometry remains as a major challenge.[5] The final product often consists of random, inhomogeneous distribution of the YAG, intermediate phases, and starting materials. Consequently, wet-chemical synthesis approaches are most often utilized because they improve homogeneity at the molecular level, leading to the formation of a single, pure YAG phase. Combustion,[6] hydrothermal,[7] precipitation,[7-9] sol-gel,[10] and spray pyrolysis[11] are some examples of wet-chemical techniques used in synthesizing the pure YAG. While some of these wet-chemical methods do require high sintering temperatures, they yield a highly crystalline pure YAG phase which results in strong luminescence.

The work presented here improved upon previously published results for synthesizing YAG derivatives. In 2000, Matsubara et al. published a direct precipitation (DP) procedure for synthesizing a chromium(III) activated YAG precursor.[9] The $Y_3Al_{5-x}Cr_xO_{12}$ (YAG: Cr^{3+}) precipitate evolved after heating a mixed metal sulfate solution with an excess of urea followed by sintering at varying

temperatures. When the phosphor was sintered at 1300 °C, the YAG structure was obtained. However, at higher sintering temperatures, the powder XRD pattern showed the presence of both the YAG and alumina (Al_2O_3). Matsubara et al. examined the YAP → YAM → YAG phase transformation at varying temperatures; however the effect of Cr^{3+} concentration on luminescence performance was not systematically investigated. Note that the chromium(III) doped YAG has a sharp, narrow band R-line at 693 nm due to the characteristic Cr^{3+} zero-phonon $^2E \rightarrow {}^4A_2$ transition. This luminescent emission can be significantly enhanced by optimizing the Cr^{3+} concentration. Therefore pursing a comprehensive study towards optimization of the level of doping is imperative to realize enhanced luminescence characteristics for many applications. In 2009, Yang et al. published an urea-based hydrothermal-precipitation (HP) process for cerium(III) activated YAG.[7a] Pure YAG phase was achieved at temperatures >1200 °C, which is 400 °C less than what is typically required using the solid-state methods.[7] To the best of our knowledge, this urea-based HP method has not been explored for synthesizing YAG: Cr^{3+}. Hence, the aim of this study was (i) to determine whether YAG: Cr^{3+} garnet can be synthesized at temperatures lower than the traditional solid-state reaction route; and (ii) whether the resulting phosphors can yield a more luminescent phosphor than using the alternative precipitation routes for two different precipitation methods (i.e. DP and HP).[7,9] Highly luminescent YAG: Cr^{3+} phosphors were achieved in this study through systematic examination of the preparation method, Cr^{3+} dopant concentration and sintering temperature.

2.0 EXPERIMENTAL SECTION

2.1 METHODS

$Y(NO_3)_3{\cdot}6H_2O$ (99.8%), $Cr(NO_3)_3{\cdot}9H_2O$ (99%), $Al(NO_3)_3{\cdot}9H_2O$ (99%), $Cr_2(SO_4)_3{\cdot}xH_2O$, and iso-propanol were purchased from Sigma-Aldrich. Urea (Certified A.C.S.) was purchased from Fisher Scientific. $Y_2(SO_4)_3{\cdot}8H_2O$ (99.9%) and $Al_2(SO_4)_3{\cdot}18H_2O$ were purchased from Alfa Aesar and Allied Chemical, respectively. The metal sulfates were dried in an oven at 120 °C for 24 h prior to use. Water was purified by using an in-house millipore water purification system. All chemicals were used as received without further treatment and/or purification.

2.2 DIRECT PRECIPITATION (DP) PREPARATION

The $Y_3Al_{5-x}Cr_xO_{12}$ powder series was synthesized by using the urea precipitation method cited by Matsubara et al.[9] The Cr^{3+} concentration of $Y_3Al_{5-x}Cr_xO_{12}$ was varied relative to Al^{3+} as x = 0.01, 0.02, 0.025, 0.05, 0.075 and 0.10 (which corresponds to 0.2 – 2 at.%) . Taking x = 0.02 (0.4 at.%) as an example, aluminum hydroxide powder was synthesized by dissolving $Al_2(SO_4)_3{\cdot}18H_2O$ (30 g, 4.50 mmol) in water (1.59 L) followed by the addition of urea (606 g, 10.09 mol). The solution was continuously stirred at 90 °C for 2 h. After cooling down to room temperature, the $Al(OH)_3{\cdot}xH_2O$ was washed and centrifuged with water (x3) and then with isopropanol (x2). The collected solid was dried at 75 °C. A portion of the $Al(OH)_3{\cdot}xH_2O$ (3.49 g, 29.4 mmol), was suspended in water (420 mL) for 2 h before adding urea (202 g, 3.36 mol). A separate solution was prepared by dissolving $Y_2(SO_4)_3{\cdot}8H_2O$ (4.18 g, 8.97 mmol) and $Cr_2(SO_4)_3{\cdot}xH_2O$ (0.117 g, 0.298 mmol) in water (220 mL). After 2 h of dissolving the metal sulfates, the $Al(OH)_3{\cdot}xH_2O$ suspension was added to the $Y_2(SO_4)_3{\cdot}8H_2O$ and $Cr_2(SO_4)_3{\cdot}xH_2O$ solution mixture. The final solution was heated at 85 °C for 1 h to precipitate the powder. After allowing the solution to cool down to room temperature, the precipitant was washed and centrifuged with water (x3) and then isopropanol (x2). The residual solid was then dried overnight in an oven at 75 °C. Powders were sintered in air (using a muffle furnace) at temperatures ranging from 1000 °C to 1600 °C in 100 °C increments for 3 h with ramp up and cool down rates of 5 °C min^{-1}.

2.3 HYDROTHERMAL-PRECIPITATION (HP) PREPARATION

The YAG: Cr^{3+} powder series was synthesized using the HP method reported by Yang et al.[7a] The molar Cr^{3+} substitution for Al^{3+} in $Y_3Al_{5-x}Cr_xO_{12}$ was varied as x = 0.01, 0.02, 0.05, 0.075, 0.10, 0.11, 0.12, 0.13, 0.14, and 0.15 (which corresponds to 0.2 – 3 at.%). Stoichiometric amounts of $Y(NO_3)_3{\cdot}6H_2O$, $Al(NO_3)_3{\cdot}9H_2O$, and $Cr(NO_3)_3{\cdot}9H_2O$ were dissolved in deionized water. The total concentration was adjusted to ~0.1 M. For instance, for the preparation of the $Y_3Al_{4.90}Cr_{0.10}O_{12}$ precursor powder, $Y(NO_3)_3{\cdot}6H_2O$ (3.45 g, 9.00 mmol), $Al(NO_3)_3{\cdot}9H_2O$ (5.63 g, 15.31 mmol), $Cr(NO_3)_3{\cdot}9H_2O$ (3 mL, 0.1 M) were dissolved in deionized water (240 mL) to give a final total concentration of ~0.1 M. Urea (5.84 g, 97.24 mmol) was then added to the aqueous mixed metal nitrate solution where the urea to nitrate molar ratio was 4:1. After 1 h of stirring at room temperature, the clear solution was distributed evenly into four 50 mL Parr Acid-Digestion Reaction Vessels. The vessels were placed into a pre-heated muffle furnace at 100 °C for 4 h. The muffle furnace was then immediately ramped to 240 °C and held at that temperature for 20 h. After allowing the vessels to cool down to room temperature, the precipitant was washed and centrifuged with water (x3) and then with isopropanol (x2). The precipitant was then dried in an oven at 75 °C overnight. Finally, the precipitant was sintered in a muffle furnace at temperatures ranging from 1000 °C to 1600 °C with 100 °C intervals in air for 3h. The temperature studies were conducted at a ramp up and cool down rate of 5 °C/min.

2.4 CHARACTERIZATION

The structure and crystallinity of the YAG: Cr^{3+} powders were measured by X-ray powder diffraction (XRD) at room temperature using Panalytical Xpert diffractometer with CuKα radiation (λ = 1.540598 Å) and X'Celerator detector. Phase identification was conducted using the HighScore Plus software and the ICDD database. The excitation (λ_{em} = 706 nm) and emission spectra (λ_{ex} = 419 and 617 nm) were obtained using a Horiba Jobin Yvon Fluorolog® spectrofluorometer equipped with a 450 W Xenon lamp as the excitation source and emission and excitation slits set at 5 nm. The CL apparatus is equipped with a RHEED 35 electron gun and RHEED 30H power supply from Staib Instruments. CL measurements were made by setting the beam acceleration voltage and electron beam current to 10 keV and 0.5 µA, respectively, at room temperature. CL spectra were acquired by an Ocean Optics HR2000 spectrometer.

3.0 RESULTS AND DISCUSSION

3.1 POWDER XRD ANALYSIS

For both synthesis approaches, the YAP → YAM → YAG phase transformation was examined as a function of sintering temperature using powder XRD. Since the DP $Y_3Al_{4.98}Cr_{0.02}O_{12}$ (YAG: 0.4 at.% Cr^{3+}) and HP $Y_3Al_{4.87}Cr_{0.13}O_{12}$ (YAG: 2.6 at.% Cr^{3+}) powders resulted in the strongest PL as function of Cr^{3+} concentration for their respective preparation method, they were selected for powder X-ray analysis. As shown in Figure 1, the DP YAG: 0.4 at.% Cr^{3+} powder consists of a crystalline mixture of the $Y_3Al_5O_{12}$ (YAG), $YAlO_3$ (YAP), and $Y_4Al_2O_9$ (YAM) phases for temperatures up to 1100 °C. Above 1200 °C, 100% conversion to the YAG phase was observed. With further increase in sintering temperature, the diffraction peak intensities become sharper as a result of the formation of a highly ordered crystalline structure. On the other hand, when the DP YAG: 0.4 at.% Cr^{3+} was sintered at even

higher temperatures, in the range of 1400 °C to 1600 °C, the diffraction peak widths remained unchanged.

The powder XRD of HP YAG: 2.6 at.% Cr^{3+} illustrated the same phase transformations as the DP processed YAG: 0.4 at.% Cr^{3+} (Figure 2). In this case, complete phase transformation to the YAG structure was also obtained for sintering temperatures >1200 °C. The powder XRD patterns for both the DP YAG: 0.4 at.% Cr^{3+} and HP YAG: 2.6 at.% Cr^{3+} sintered at various temperatures confirm that the YAG: Cr^{3+} garnet can be synthesized at temperatures lower than the traditional solid-state reaction route (i.e., T = 1600 °C).

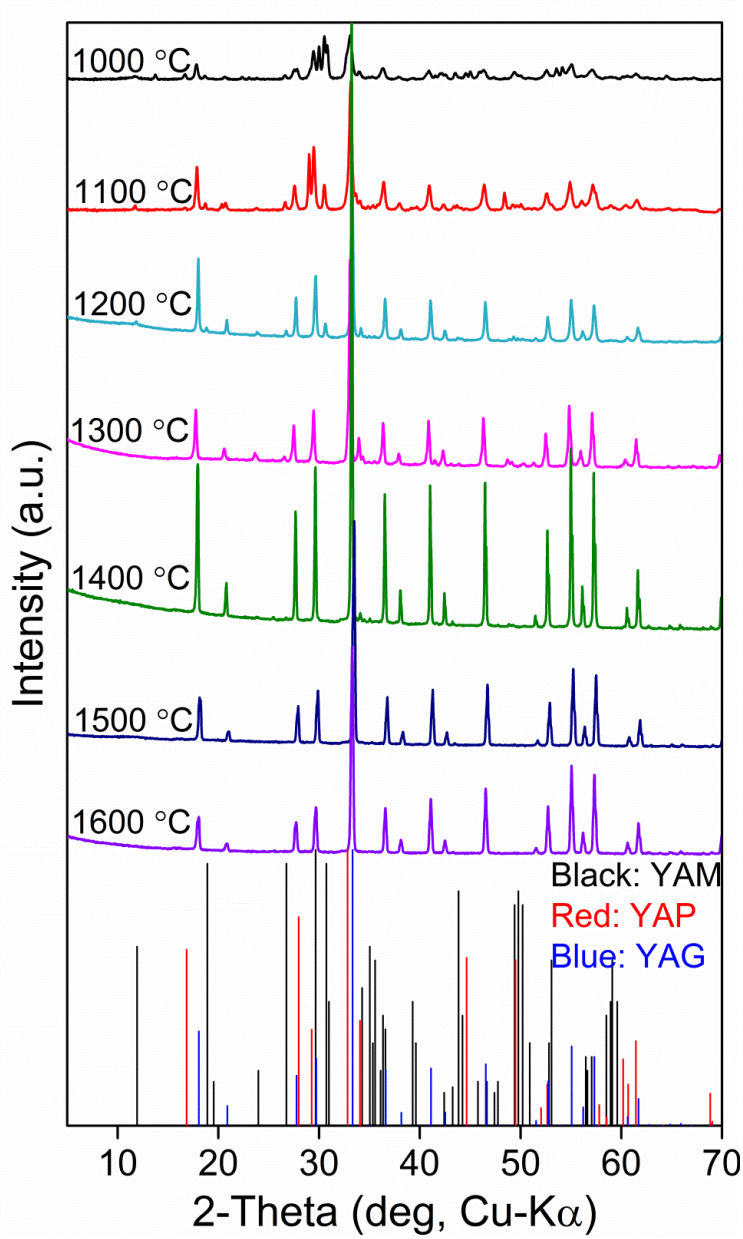

Figure 1. Powder XRD patterns of the DP YAG: 0.4 at.% Cr^{3+} powder at various sintering temperatures. Lower panel in black: YAM PDF#00-022-0987, red: YAP PDF#01-074-1334, and blue: YAG PDF#01-075-6655.

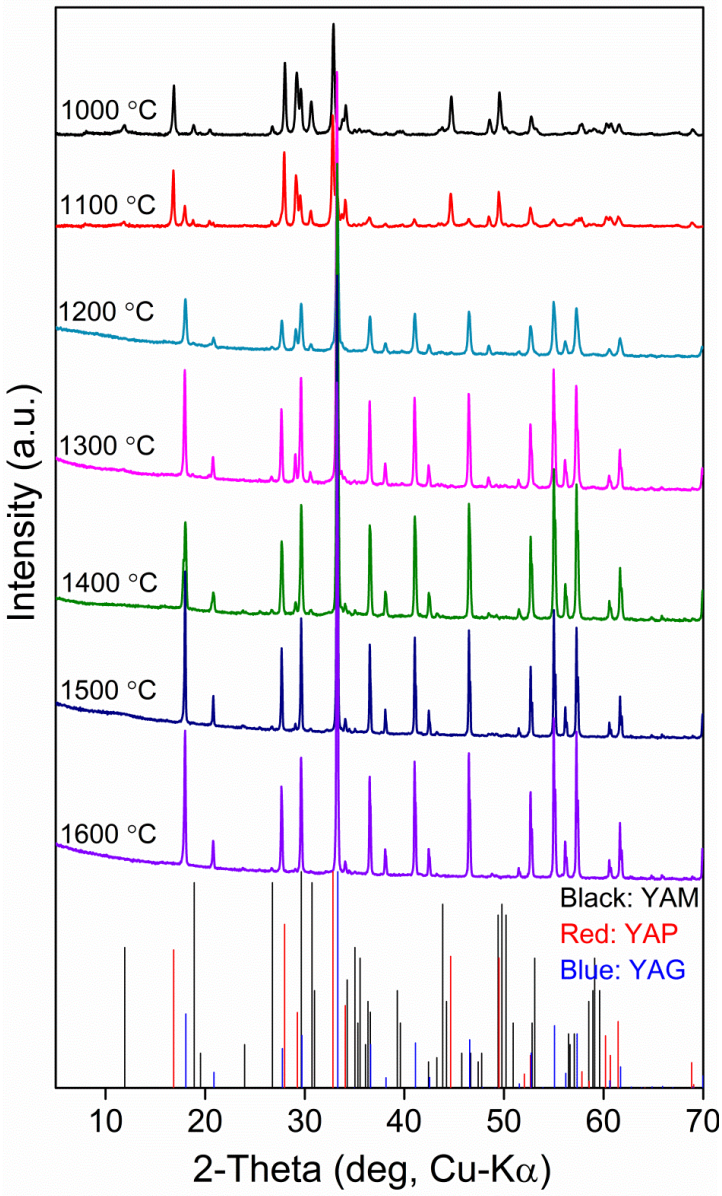

Figure 2. Powder XRD patterns of the HP YAG: 2.6 at.% Cr^{3+} powder at various sintering temperatures. Lower panel in black: YAM PDF#00-022-0987, red: YAP PDF#01-074-1334, and blue: YAG PDF#01-075-6655.

3.2 PHOTOLUMINESCENCE (PL)

The excitation and emission spectra of the DP YAG: 0.4 at.% Cr^{3+} and HP YAG: 2.6 at.% Cr^{3+} were measured and are shown in Figure 3. Both methodologies produced compounds with Cr^{3+} spin allowed $^4A_2 \rightarrow {}^4T_1$ and $^4A_2 \rightarrow {}^4T_2$ excitation transitions at 419 and 617 nm, respectively.[8,12] Four pronounced bands at 677, 693, 706, and 725 nm were observed in the emission spectra. The sharp R-line at 693 nm is a result of the Cr^{3+} zero-phonon $^2E \rightarrow {}^4A_2$ transition,[8,12] while its associated Stokes phonon sidebands are near 706 and 725 nm. An anti-Stokes phonon sideband was observed at 677 nm.[8] As the sintering temperature was increased, the PL emission band became broader at longer wavelengths. This

broadening effect is associated with the $^4T_2 \rightarrow {}^4A_2$ emission band which resides under the R-line. The DP and HP approaches had similar PL intensities when both were sintered at 1600 °C.

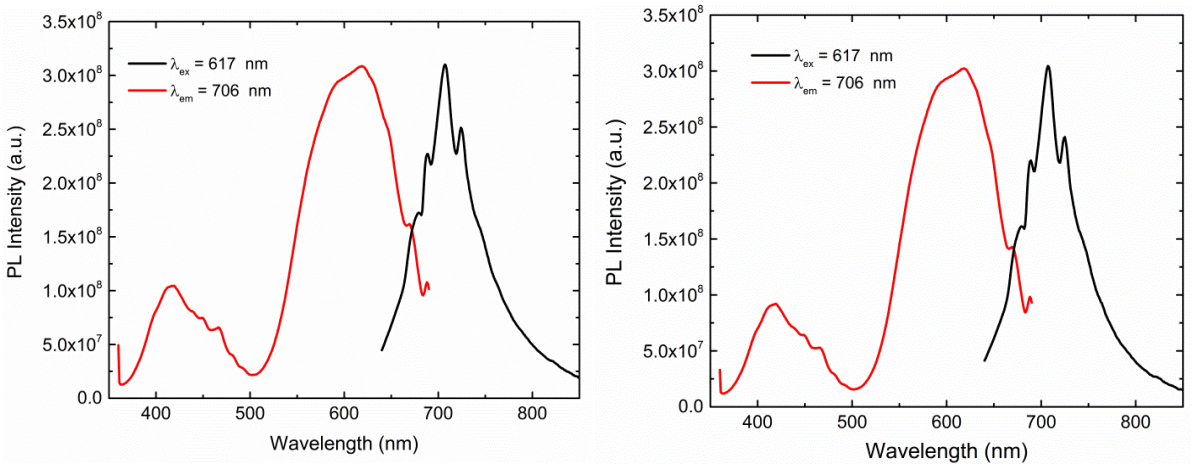

Figure 3. Excitation (λ_{em} = 706 nm) and emission spectra (λ_{ex} = 617 nm) of (a) DP YAG: 0.4 at.% Cr^{3+} and (b) HP YAG: 2.6 at.% Cr^{3+} powders sintered at 1600 °C.

The PL emission intensity of the DP YAG: 0.4 at.% Cr^{3+} was studied as a function of wavelength excitation (Figure 4). The dependency of the PL light output was compared by using the integrated intensity of the R-line transition. The relative PL integrated intensity values were normalized to the best performing sample (excited at 617 nm) - the phosphor sintered at 1600 °C. As predicted, the PL emission intensity improved as sintering temperature increased when using either excitation bands (419 or 617 nm). This observation is expected due to the phase transformation from the YAM→YAP→YAG.

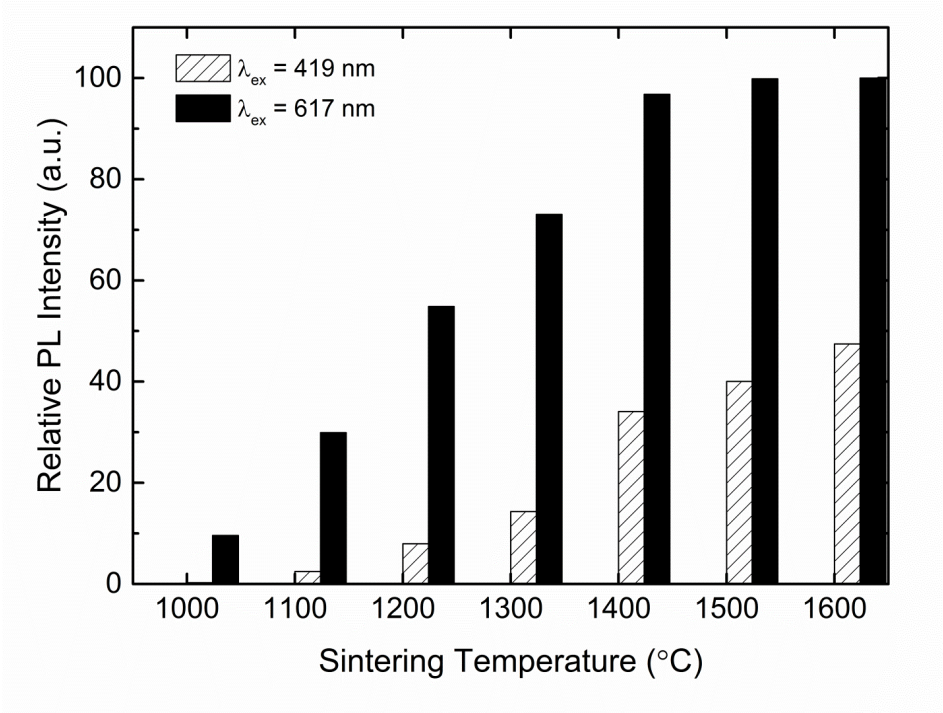

Figure 4. PL intensity as a function of excitation wavelength of the YAG: 0.4 at.% Cr^{3+} prepared via DP.

Figure 5 shows the PL intensity as a function of the Cr^{3+} concentration. Similar to the dependency of the excitation wavelength, the PL data for all samples was compared using the integrated intensity of the R-line transition, and the relative emission intensity values were normalized to the best performing sample. It is clear that for both preparation routes, once the Cr^{3+} concentration was optimized, the PL emission intensities were observed to be very similar (Figure 3). In addition, our study exemplifies how different synthesis techniques have an effect on the concentration quenching of Cr^{3+} in the YAG phosphor. The PL efficiency of the DP YAG: Cr^{3+} at its quenching concentration (0.4 at.%) was equal to that of the HP YAG: Cr^{3+} at its quenching concentration (2.6 at.%). For the case of HP YAG: Cr^{3+} phosphor, as the Cr^{3+} concentration increased from 0.2 to 2.6 at.%, the PL emission intensity was also amplified. Note that the saturation state of the PL intensity for the HP YAG: Cr^{3+} phosphor is observed to be higher than the DP YAG: Cr^{3+} phosphor. In fact, at higher Cr^{3+} concentrations (> 2.6 at.%), the HP YAG: Cr^{3+} luminescence emission intensity was drastically diminished.

In general, the quenching of the PL is caused by the cross-relaxation and energy transfer between a pair of Cr^{3+} activators.[13] The cross-relaxation phenomena occurs when the excited Cr^{3+} electron relaxes into one of its own lower energy Cr^{3+} excited states rather than to its Cr^{3+} ground state. Most often the concentration quenching effect occurs at high dopant concentration levels due to the large degree of interaction between Cr^{3+} ions resulting from the Cr^{3+}-Cr^{3+} distance decreasing. Subsequently, the energy transfer rate between closely spaced Cr^{3+} ions and energy transfer to traps or quenching sites increases. Consequently, in both quenching scenarios, the Cr^{3+} emission will either be absent or diminish. From these two phenomena, this would imply the DP synthesis technique resulted in a more effective energy transfer rate than the HP approach at low Cr^{3+} concentration levels. Hence the difference in the Cr^{3+} optimization for each synthesis method can be associated to the relative distance between two Cr^{3+} ions. Based upon our findings, additional experiments such as studying how the particle-size and morphology relates to the Cr^{3+} concentration quenching effect would be worthwhile to investigate.

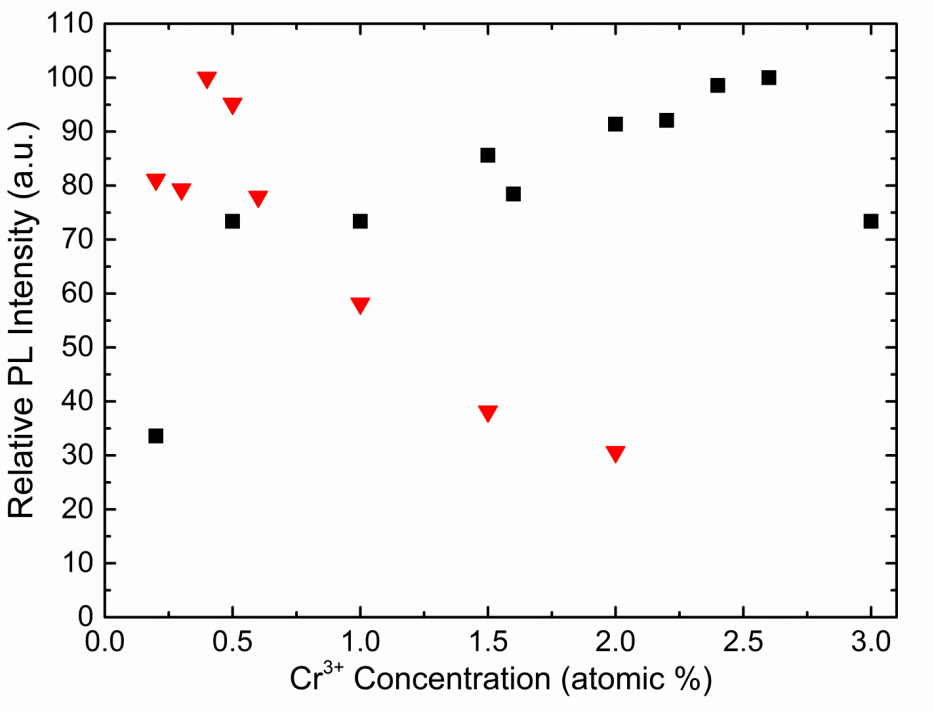

Figure 5. PL intensity as a function of Cr^{3+} concentration for the YAG: Cr^{3+} prepared by using (■) DP and (▼) HP at 1600 °C.

Next we illustrate the effect of sintering temperature (for each method) on the PL performance for optimum doped YAG: Cr^{3+} samples (Figure 6). The PL results were compared using the integrated intensity of the R-line transition. As the sintering temperature increased from 1000 to 1400 °C, the PL intensity increased linearly for both synthesis approaches. Above 1400 °C, while the same trend continued for the HP samples, saturation in PL intensity is observed for the DP processed samples. This indicates that, for the latter, no additional phase transformations or compositional changes occur above 1400 °C, which also agrees with the XRD observations. In addition, the PL yield of the DP YAG: 0.4 at.% Cr^{3+} was slightly greater than the HP YAG: 2.6 at.% Cr^{3+} up to 1500 °C. This demonstrates that the HP YAG: 2.6 at.% Cr^{3+} powder required higher elevated sintering temperatures (>1400 °C) to obtain the same photoluminescence output as the DP YAG: 0.4 at.% Cr^{3+} sample exhibited at 1400 °C. These results clearly demonstrate the differences between processing approaches for the fabrication of a high performance luminescent material.

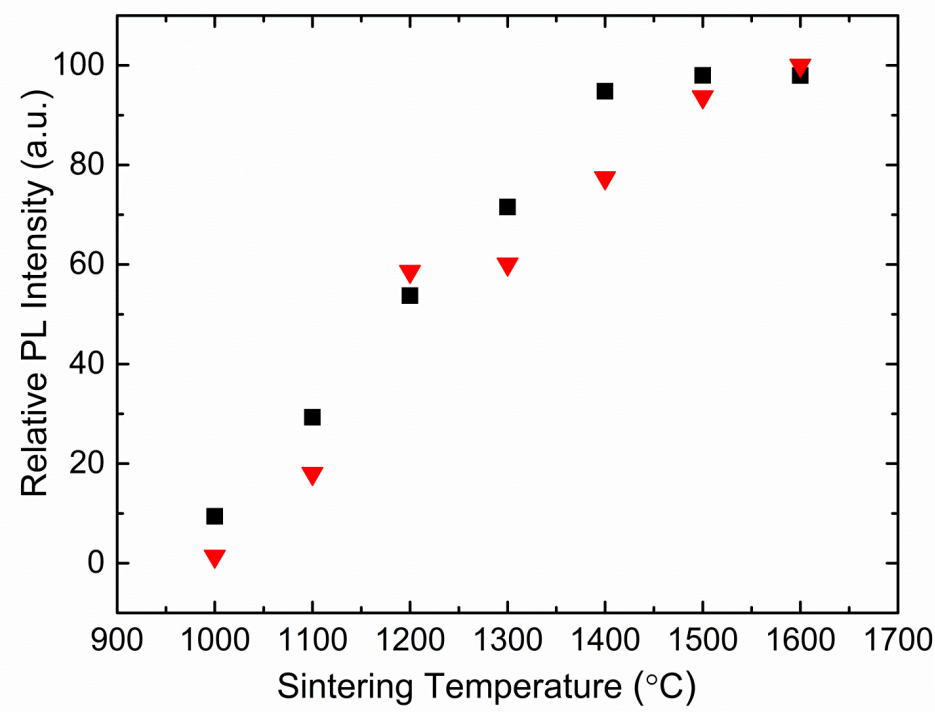

Figure 6. PL intensity as a function of sintering temperature of the (■) direct precipitation YAG: 0.4 at.% Cr^{3+} and (▼) hydrothermal-precipitation YAG: 2.6 at.% Cr^{3+}.

3.3 CATHODOLUMINESCENCE (CL)

Figure 7 demonstrates the CL emission dependency on the Cr^{3+} concentration for the DP YAG: Cr^{3+} phosphors when sintered at 1600 °C. The integrated intensity (see inset) of the Cr^{3+} zero-phonon $^2E \rightarrow {}^4A_2$ transition was used to evaluate the CL results. The YAG: Cr^{3+} CL emission band illustrated the same characteristic Cr^{3+} transitions as observed in the PL emission.[8a] As anticipated, the CL results were in agreement with the PL findings, where the CL emission intensity reached a maximum at 0.4 at% Cr^{3+} and then decreased substantially as the Cr^{3+} concentration increased beyond the 0.6 at.% Cr^{3+}.

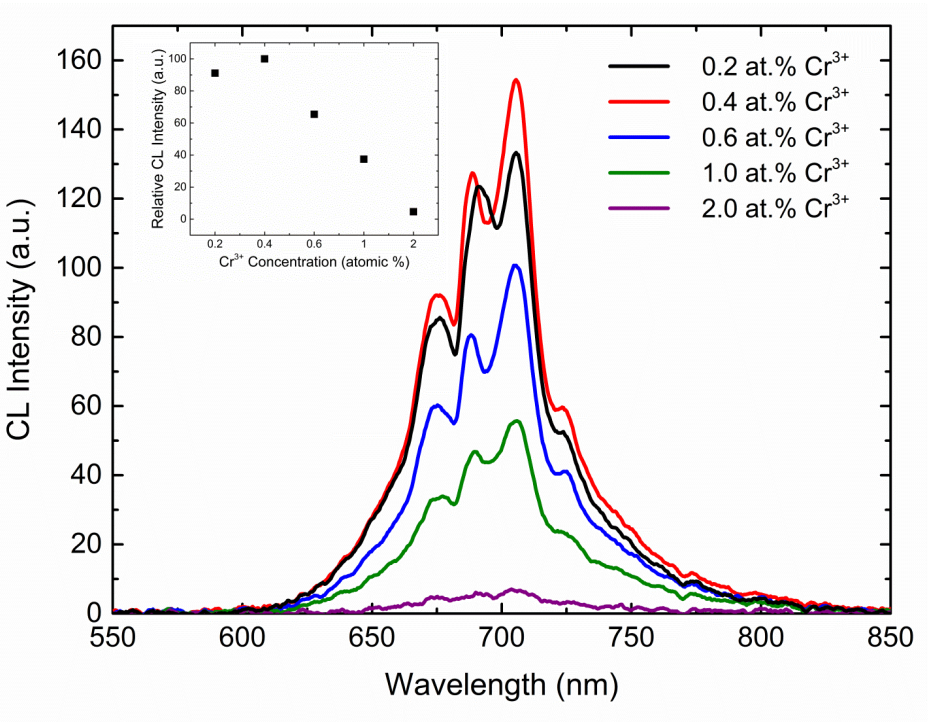

Figure 7. CL spectra illustrating the CL intensity as a function of Cr^{3+} concentration of the DP YAG: Cr^{3+} sintered at 1600 °C. Inset: Integrated CL emission.

4.0 CONCLUSIONS

This work demonstrates that more than one wet-chemical approach can be utilized to derive a given phosphor system (e.g. YAG: Cr^{3+}) which can yield a similar PL emission intensity. We explored two preparation routes, direct precipitation and hydrothermal precipitation. The photoluminescence emission intensities were similar once the Cr^{3+} dopant concentration and sintering temperature were optimized for both preparation methods. Thus, the PL efficiency of the DP YAG: Cr^{3+} was equal to that of the HP YAG: Cr^{3+} when the Cr^{3+} concentration / sintering temperature was 0.4 at.% / 1400 °C and 2.6 at.% / 1600 °C, respectively. In addition, the DP YAG: 0.4 at.% Cr^{3+} phosphors showed the strongest CL emission intensity. The combined findings of CL and PL studies indicate the DP processed red phosphor (YAG: Cr^{3+}) has significant potential for applications not only as a phosphor coating on light emitting diodes but also in cathode ray tubes, solar-cells,[14] plasma display panels,[15] solid-state lasers,[16] and medical imaging.[17]

5.0 REFERENCES

[1] i.e., (a) Wu, H.; Zhang, X.; Guo, C.; Xu, J.; Wu, M.; Su, Q. Three-band White Light from InGaN-Based Blue LED Chip Precoated with Green/Red Phosphors IEEE Photonics Technol. Lett. 2005, 17, 1160-1162. (b) Pust, P.; Weiler, V.; Hecht, C.; Tuecks, A.; Wochnik, A. S.; Henss, A.-K.; Wiechert, D.; Scheu, C.; Schmidt, P. J.; Schnick, W. Narrow-Band Red-Emitting $Sr[LiAl_3N_4]:Eu^{2+}$ as a Next-Generation LED-Phosphor Material. Nat. Mater. 2014, 13, 891-896. (c) Guo, Y.; Sun, M.; Guo, W.; Ren, F.; Chen, D. Luminescent Properties of Eu^{3+} Activated Tungstate Based Novel Red-Emitting Phosphors.

Opt. Laser Technol. 2010, 42, 1328-1331. (d) Jang, H. S.; Im, W. B.; Lee, D. C.; Jeon, D. Y.; Kim, S. S. Enhancement of Red Spectral Emission Intensity of $Y_3Al_5O_{12}:Ce^{3+}$ Phosphor via Pr Co-Doping and Tb Substitution for the Application to White LEDs. J. Lumin. 2007, 126, 371-377. (e) Jang, H. S.; W., Y.-H.; Jeon, D. Y. Improvement of Electroluminescent Property of Blue LED Coated with Highly Luminescent Yellow-Emitting Phosphors. Appl. Phys. B: Lasers Opt. 2009, 95, 715-720.

[2] (a) Mueller-Mach, R.; Mueller, G. O. White-Light-Emitting Diodes for Illumination. Proc. of SPIE 2000, 3938, 30-41. (b) Smet, P. F.; Parmentier, A. B.; Poelman, D. Selecting Conversion Phosphors for White Light-Emitting Diodes. J. Electrochem. Soc. 2011, 158, R37-R54. (c) Krames, M. R.; Shchekin, O. B.; Mueller-Mach, R.; Mueller, G. O.; Zhou, L.; Harbers, G.; Craford, M. G. Status and Future of High-Power Light-Emitting Diodes for Solid-State Lighting. J. Disp. Technol. 2007, 3, 160-175

[3] i.e., (a) Ohno, K.; Abe, T. Bright green phosphor, terbium-activated aluminum gallium yttrium oxide ($Y_3Al_{5-x}Ga_xO12:Tb$), for projection CRT. J. Electrochem. Soc. 1987, 134, 2072-2076. (b) Choe, J.Y.; Ravichandra, D.; Blomquist, S.M.; Kirchner, K.M.; Forsythe, E.W.; Morton, D.C. Cathodoluminescence Study on Novel Sol-Gel Derived $Y_{3-x}Al_5O_{12}:Tb_x$ Phosphors J. Lumin. 2001, 93, 119-128. (c) Choe, J.Y.; Ravichandra, D.; Blomquist, S.M.; Morton, D.C.; Kirchner, K.M.; Ervin, M.H.; Lee, U. Alkoxy Sol-Gel Derived $Y_{3-x}Al_5O_{12}:Tb_x$ Thin Films as Efficient Cathodoluminescent Phosphors. Appl. Phys. Lett. 2001, 78, 3800-3802. (d) Autrata, R.; Schauer, P.; Kvapil, Jo.; Kvapil, Ji. Cathodoluminescent Efficiency of $Y_3Al_5O_{12}$ and $YAlO_3$ Single Crystals in Dependence on Ce^{3+} and Other Dopants Concentrations. Cryst. Res. Technol. 1983, 18, 907-913. (e) Robbins, D.J.; Cockayne, B.; Lent, B.; Glasper, J.L. The relationship Between Concentration and Efficiency in Rare Earth Activated Phosphors. J. Electrochem. Soc. 1979, 126, 1556-1563.

[4] i.e., (a) Jia, D.; Wang, Y.; Guo, X.; Li, K.; Zou, Y.K.; Jia, W. Synthesis and Characterization of YAG: Ce^{3+} LED Nanophosphors. J. Electrochem. Soc. 2007, 154, J1-J4. (b) Raue, R.; Vink, A.T.; Welker, T. Phosphor Screens in Cathode-Ray Tubes for Projection Television. Philips Tech. Rev. 1989, 44, 335-347. (c) Lee, S.; Seo, S.Y. Optimization of Yttrium Aluminum Garnet:Ce^{3+} Phosphors for White Light-Emitting Diodes by Combinatorial Chemistry Method. J. Electrochem. Soc. 2002, 149, J85-J88. (d) Milosevic, O.; Mancic, L.; Rabanal, M.E.; Torralba, J.M.; Yang, B.R.; Townsend, P. Structural and Luminescence Properties of $Gd_2O_3:Eu^{3+}$ and $Y_3Al_5O_{12}:Ce^{3+}$ Phosphor Particles Synthesized via Aerosol. J. Electrochem. Soc. 2005, 152, G707-G713. (e) Chung, Y.S.; Kang, Y.C.; Park, S.B. Luminescence and CL Saturation Characteristics of Eu doped Y-Al-O Multicomposition Phosphor Prepared by Spray Pyrolysis. J. Electrochem. Soc. 2004, 151, H180-H183.

[5] (a) Pan, Y.; Wu, M.; Su, Q. Comparative Investigation on Synthesis and Photoluminescent of YAG:Ce Phopshor. Mater. Sci. Eng. B. 2004, 106, 251-256. (b) Pan, Y.; Wu, M.; Su, Q. Taiolored Photoluminescenec of YAG: Ce Phosphor Through Various Methods. J. Phys. Chem. Solids. 2004, 65, 845-850. (c) Hess, N.J.; Maupin, G.D.; Chick, L.A.; Sunberg, D.S.; McCreedy, D.E.; Armstrong, T.R. Synthesis and Crystallization of Yttrium-Aluminum Garnet and Related Compounds. J. Mater. Sci. 1994, 29, 1873-1878.

[6] (a) Fu, Y.-P.; Tsao, S.; Hu, C.-T. Preparation of Y3Al5O12:Cr powders by Microwave-Induced Combustion Process and Their Luminescent Properties. J. Alloys Compd. 2005, 395, 227-230. (b) Blosi, M.; Albonetti, S.; Dondi, M.; Costa, A.L.; Ardit, M.; Cruciani, G. Sol-Gel Combustion Synthesis of Chromium Doped Yttrium Aluminum Perovskites. J. Sol-Gel Sci. Technol. 2009, 50, 449-455. (c) Gupta, K.V.K.; Muley, A.; Yadav, P.; Joshi, C.P.; Moharil, S.V. Combustion Synthesis of YAG: Ce and Related Phosphors. Appl. Phys. B. 2005, 105, 479-484. (d) Laishram, K.; Mann, R.; Malhan, N. Single Step Synthesis of Yttrium Aluminum Garnet ($Y_3Al_5O_{12}$) Nanopowders by Mixed Fuel Solution Combustion Approach. Ceram. Int. 2011, 37, 3743-3746. (e) Xia, G.; Zhou, S.; Zhang, J.; Xu, J. Structural and Optical Properties of YAG:Ce^{3+} Phosphors by Sol–Gel Combustion Method. J. Cryst. Growth. 2005, 279, 357-

362. (f) Qiu, F.; Pu, X.; Li. J.; Liu, X.; Pan, Y.; Guo, Thermal Behavior of the YAG Precusor Prepared by Sol-Gel Combustion Process. J. Ceram. Int. 2005, 31, 663-665. (g) Li, J.; Pan, Y.; Qiu, F.; Wu, Y.; Liu, W.; Guo, J. Synthesis of Nanosized Nd:YAG Powders via Gel Combustion. Ceram. Int. 2007, 33, 1047-1052. (h) Gowda, G. J. Mater. Sci. Lett. Synthesis of Yttrium Aluminates by the Sol-Gel Process. 1986, 5, 1029-1032.

[7] (a) Yang, H.; Yuan, L.; Zhu, G.; Yu, A.; Xu, H. Luminescent properties of YAG: Ce3+ Phosphor Powders Prepared by Hydrothermal-Homogenous Precipitation Method. Mater. Lett. 2009, 63, 2271-2273. (b) Hoghooghi, B.; Healey, L.; Powell, S.; McKittrick, J.; Sluzky, E.; Hesse, K. Synthesis of YAG:Cr Phosphors by Precipitation from Aluminum and Yttrium Sulfate Solutions. Mater. Chem. Phys. 1994, 38, 175-180.

[8] (a) Gluchowski, P.; Pazik, R.; Hreniak, D.; Strek, W. Luminescence properties of Cr^{3+}: $Y_3Al_5O_{12}$ nanocrystals. J. Lumin. 2009, 129, 548-553. (b) Shen, Y. R.; Bray, K. L. Effect of Pressure and Temperature on the Lifetime of Cr^{3+} in Yttrium Aluminum Garnet. Phys. Rev. B. 1997, 56, 10882. (c) Hehir, J. P.; Henry, M. O.; Larkin, J. P.; Imbusch, G. F. Nature of the Luminescence from Chromium(3+) -doped YAG. J. Phys. C: Solid State Phys. 1974, 7, 2241-2248. (d) Kinsman, K. M.; McKittrick, J. Phase Development and Luminescence in Chromium-Doped Yttrium Aluminum (YAG: Cr) Phosphors. JACS, 1994, 77, 2866-2872.
[9] Matsubara, I.; Paranthaman, M.; Allison, S.W.; Cates, M.R.; Beshears, D.L.; Holcomb, D.E. Preparation of Cr-Doped $Y_3Al_5O_{12}$ Phosphors by Heterogeneous Precipitation Methods and Their Luminescent Properties. Mater. Res. Bull. 2000, 35, 217-224.

[10] (a) Skaudziu, R.; Pinkas, J.; Raudonis, R.; Selskis, A.; Juskenas, R.; Kareiva, A. On the Limitary Radius of Garnet Structure Compounds $Y_3Al_{5-x}M_xO_{12}$ (M = Cr, Co, Mn, Ni, Cu) and $Y_3Fe_{5-x}Co_xO12$ ($0 \leq x \leq 2.75$) Syntehsized by Sol-Gel Method. Mater. Chem. Physics. 2012, 135, 479-485. (b) Fujioka, K.; Saiki, T.; Motokoshi, S.; Fujimoto, Y.; Fujita, H.; Nakatsuka, M. Pre-Evaluation Method for the Spectroscopic Properties of YAG Bulk Materials by Sol–Gel Synthetic YAG Powder. Ceram. Int. 2009, 35, 2393-2399. (c) Muliuoliene, I.; Mathur, S.; Jasaitis, D.; Shen, H.; Sivakov, V.; Rapalaviciute, R.; Beganskiene, A.; Kareiva, A. Evidence of the Formation of Mixed-Metal Garnets via Sol-Gel Synthesis. Opt. Mater. 2003, 22, 241-250.

[11] (a) Kang, Y.B.; Lenggoro, I.W.; Park, S.B.; Okuyama, K. YAG:Ce Phosphor Particles Prepared by Ultrasonic Spray Pyrolysis. Mater. Res. Bull. 2000, 35, 789-798. (b) Purwanto, A.; Wang, W.-N.; Ogi, T.; Lenggoro, W.; Tanabe, E.; Okuyama, K. High Luminance YAG:Ce Nanoparticles Fabricated from Urea Added Aqueous Precursor by Flame Process. J. Alloys Compd. 2008, 463, 350-357. (c) Wang, W.-N.; Kim, S.-G.; Lenggoro, W.; Okuyama, K. Polymer-Assisted Annealing of Spray-Pyrolyzed Powders for Formation of Luminescent Particles with Submicrometer and Nanometer Sizes. J. Am. Ceram. Soc. 2007, 90, 425-432.

[12] (a) Deren, P.J.; Watras, A.; Gagor, A.; Pazik, R. Weak Crystal Field in Yttrrium Gallium Garnet (YGG) Submicrocrystals Doped with Cr^{3+}. Cryst. Growth Des. 2012, 12, 4752-4757. (b) Sugimoto, A.; Nobe, Y.; Yamagishi, K. Crystal Growth and Optical Characterization of Cr,Ca: $Y_3Al_5O_{12}$. J. Cryst. Growth. 1994, 140, 349-354.

[13] Jia, D.; Lewis, L.A.; Wang, X.-J. Cr^{3+}-Doped Lanthanum Gallogermanate Phosphors with Long Persistent IR Emission. Electrochem. Solid-State Lett. 2010, 13, J32-J34.

[14] i.e., (a) Hosseini, Z.; Huang, W.-K.; Tsai, C.-M.; Chen, T.-M.; Taghavinia, N.; Diau, E. W.-G. Enhanced Light Harvesting with a Reflective Luminescent Down-Shifting Layer for Dye-Sensitized Solar Cells. ACS Appl. Mat. Interfaces, 2013, 5, 5397-5402. (b) Kuo, T.-W.; Liu, W.-R.; Chen, T.-Ming. High

Color Rendering White Light-Emitting-Diode Illuminator using the Red-Emitting Eu^{2+}-Activated CaZnOS Phosphors Excited by Blue LED. Opt. Express 2010, 18, 8187-8192.

[15] i.e., (a) Yadav, R.; Khan, A. F.; Yadav, A.; Chander, H.; Haranath, D.; Gupta, B. K.; Shanker, V.; Chawla, S. Intense Red-Emitting $Y_4Al_2O_9:Eu^{3+}$ Phosphor with Short Decay Time and High Color Purity for Advanced Plasma Display Panel. Opt. Express 2009, 17, 22023-22030. (b) Lai, H.; Chen, B.; Xu, W.; Xie, Y.; Wang, X,; Di, W. Fine Particles $(Y,Gd)P_xV_{1-x}O_4:Eu^{3+}$ Phosphor for PDP Prepared by Coprecipitation Reaction. Mat. Lett. 2006, 60, 1341-1343. (c) Yang, H. M.; Shi, J. X.; Gong, M. L. A Novel Red Emitting Phosphor $Ca_2SnO_4:Eu^{3+}$. J. Solid State Chem. 2005, 178, 917-920.

[16] i.e., Ikesue, A.; Kamata, K.; Yoshida, K. Synthesis of Nd^{3+},Cr^{3+}-Codoped YAG Ceramics for High-Efficiency Solid-State Laers. J. Am. Ceram. Soc. 1995, 78, 2545-2547.

[17] i.e., (a) Allen, P. M.; Liu, Wenhao; C., Vikash P.; Lee, J.; Ting, A. Y.; Fukumura, D.; Jain, R. K.; Bawendi, M. G. InAs(ZnCdS) Quantum Dots Optimized for Biological Imaging in the Near-Infrared. JACS 2010, 132, 470-471. (b) Tous, J.; Horvath, M.; Pina. L.; Blazek, K.; Sopko, B. High-Resolution Application of YAG:Ce and LuAG:Ce Imaging Detectors with a CCD X-Ray Camera. Nucl. Instrum. Methods Phys. Res., Sect. A 2008, 591, 264-267. (c) Tous, J.; Horodysky, P.; Blazek, K.; Nikl, M.; Mares, J. A. High Resolution Low Energy X-Ray Microradiography using a CCD Camera. J. Instrum. 2011, 6, C01048/1-C01048/6.

INTERNAL DISTRIBUTION

1. Tolga Aytug
2. Case Collins
3. Linda A. Lewis
4. Brenda Smith
5. Cyril Thompson
6. ORNL Office of Technical Information

EXTERNAL DISTRIBUTION

1. Calvin Shipbaugh
2. Reza Dabestani